International Journal of
Molecular Sciences

MDPI

Article

Xanthine Oxidoreductase-Mediated Superoxide Production Is Not Involved in the Age-Related Pathologies in *Sod1*-Deficient Mice

Shuichi Shibuya [1], Kenji Watanabe [1], Yusuke Ozawa [2] and Takahiko Shimizu [1,2,*]

[1] Aging Stress Response Research Project Team, National Center for Geriatrics and Gerontology, Obu, Aichi 474-8511, Japan; s-shibuya@ncgg.go.jp (S.S.); kng-wtnb@ncgg.go.jp (K.W.)
[2] Department of Endocrinology, Hematology, and Geriatrics, Chiba University Graduate School of Medicine, Chiba, Chiba 260-8670, Japan; ozawayusuke3@gmail.com
* Correspondence: shimizut@ncgg.go.jp; Tel.: +81-562-44-5651; Fax: +81-562-48-2373

Abstract: Reactive oxygen species (ROS) metabolism is regulated by the oxygen-mediated enzyme reaction and antioxidant mechanism within cells under physiological conditions. Xanthine oxidoreductase (XOR) exhibits two inter-convertible forms (xanthine oxidase (XO) and xanthine dehydrogenase (XDH)), depending on the substrates. XO uses oxygen as a substrate and generates superoxide ($O_2^{\bullet-}$) in the catalytic pathway of hypoxanthine. We previously showed that superoxide dismutase 1 (SOD1) loss induced various aging-like pathologies via oxidative damage due to the accumulation of $O_2^{\bullet-}$ in mice. However, the pathological contribution of XO-derived $O_2^{\bullet-}$ production to aging-like tissue damage induced by SOD1 loss remains unclear. To investigate the pathological significance of $O_2^{\bullet-}$ derived from XOR in *Sod1*$^{-/-}$ mice, we generated *Sod1*-null and XO-type- or XDH-type-knock-in (KI) double-mutant mice. Neither XO-type- nor XDH-type KI mutants altered aging-like phenotypes, such as anemia, fatty liver, muscle atrophy, and bone loss, in *Sod1*$^{-/-}$ mice. Furthermore, allopurinol, an XO inhibitor, or apocynin, a nicotinamide adenine dinucleotide phosphate oxidase (NOX) inhibitor, failed to improve aging-like tissue degeneration and ROS accumulation in *Sod1*$^{-/-}$ mice. These results showed that XOR-mediated $O_2^{\bullet-}$ production is relatively uninvolved in the age-related pathologies in *Sod1*$^{-/-}$ mice.

Keywords: superoxide; SOD1; xanthine oxidoreductase; aging; oxidative stress

Citation: Shibuya, S.; Watanabe, K.; Ozawa, Y.; Shimizu, T. Xanthine Oxidoreductase-Mediated Superoxide Production Is Not Involved in the Age-Related Pathologies in *Sod1*-Deficient Mice. *Int. J. Mol. Sci.* **2021**, *22*, 3542. https://doi.org/10.3390/ijms22073542

Academic Editor: Maria Luisa Balestrieri

Received: 19 February 2021
Accepted: 24 March 2021
Published: 29 March 2021

1. Introduction

In mammalian cells, several mechanisms or pathways are associated with the production of reactive oxygen species (ROS), including superoxide ($O_2^{\bullet-}$), within cells under physiological and pathological conditions. These include mitochondrial respiration, xanthine oxidoreductase (XOR), and nicotinamide adenine dinucleotide phosphate (NADPH) oxidase (NOX) [1,2]. Redox balance is physiologically maintained by the production and degradation of ROS by antioxidants, including vitamins C and E, and enzymes, such as superoxide dismutase (SOD), catalase, and glutathione peroxidase, in the cellular system.

To better understand the intracellular redox regulation, gene modification studies have been performed. Accumulating evidence has demonstrated that *Sod1*-deficient (*Sod1*$^{-/-}$) mice show complete SOD1 protein loss and increased intracellular $O_2^{\bullet-}$ as well as various aging-associated organ pathologies, such as hepatic carcinoma [3], fatty liver [4], acceleration of Alzheimer's disease [5,6], macular degeneration [7,8], dry eye [9,10], hemolytic anemia [11], osteopenia [12,13], skin atrophy [14,15], skeletal muscle atrophy [16], luteal degeneration [17], and alteration of the gastrointestinal microbiota [18]. SOD1 loss leads to the accumulation of oxidative molecules, including lipid peroxides, carbonylated proteins, oxidized nucleic acids, and advanced glycation end products, which results in widespread impaired cellular signaling, gene expression, and cell death in tissues [19]. Therefore, SOD1 plays a central role in cytoplasmic $O_2^{\bullet-}$ metabolism in intracellular redox regulation.

Mammalian XOR is ubiquitously expressed and catalyzes the conversion of hypoxanthine to xanthine and xanthine to uric acid. XOR can be found in two inter-convertible forms: (1) xanthine oxidase (XO) is an $O_2^{\bullet-}$-mediated type that uses oxygen and generates $O_2^{\bullet-}$, while (2) xanthine dehydrogenase (XDH) is an NAD^+-mediated type that uses NAD^+ as a cofactor and leads to reduced nicotinamide adenine dinucleotide production but not the generation of $O_2^{\bullet-}$ [20]. These two types of XOR differ in the structure of the active site loop and the loop containing flavin adenine dinucleotide and molybdenum domains [21]. Pharmacological intervention with XO inhibitors has shown that XO is involved in various acute-injury models, such as ischemia-reperfusion injury [22,23], hyperglycemic cardiomyopathy [24], and neurodegeneration induced by spinal cord injury [25]. These results suggest that XO-mediated $O_2^{\bullet-}$ production impairs organ integrity under pathological conditions. Since XOR-knockout mice die within six weeks after birth due to renal failure [26], it is difficult to elucidate the role of XOR in vivo. To clarify the pathophysiological contribution of XOR, Kusano et al. generated two types of knock-in (KI) mice for XO-locked- or XDH-stable KI mutations [21]. The XO-locked-type mice that generate $O_2^{\bullet-}$, but not the XDH-stable-type mice that do not generate $O_2^{\bullet-}$, showed markedly increased tumor growth associated with the activation of macrophages [21]. However, the distinct roles of XO or XDH in aging-like pathologies induced by SOD1 deficiency remain unclear.

In the present study, to investigate the pathological significance of XOR-mediated $O_2^{\bullet-}$ in *Sod1*$^{-/-}$ mice, we generated SOD1 and XO-locked type- or XDH-stable-type KI double-mutant mice and investigated the pathological association between XO-produced $O_2^{\bullet-}$ and age-related pathologies caused by SOD1 deficiency. Furthermore, we administered XOR or NOX inhibitors to *Sod1*-deficient mice and investigated the protective effect of suppression of XO- and NOX-derived $O_2^{\bullet-}$ on the aging-like phenotypes induced by oxidative stress.

2. Results

2.1. XO-Locked or XDH-Stable Types Failed to Improve the Aging-Like Phenotypes of Sod1$^{-/-}$ *Mice*

Since the physiological and pathological roles of XO/XDH conversion remain controversial, we used XO-locked-type mutant mice (W338A/F339L) to elucidate the pathological role in XO-derived $O_2^{\bullet-}$ in vivo [21,27]. To confirm the contribution of XO to the phenotypes of *Sod1*$^{-/-}$ mice, we generated *Sod1*$^{-/-}$ XO-locked-type double-mutant mice (Figure 1). *Sod1*$^{-/-}$ XO-locked-type mice were born according to the Mendelian rule without lethality, showing no apparent growth abnormalities (data not shown). As with *Sod1*$^{-/-}$ mice, the *Sod1*$^{-/-}$ XO-locked-type double-mutant mice also showed reduced red blood cells and splenomegaly (Figure 1A,B). The XO-locked type did not further exacerbate the progression of fatty liver, muscle atrophy, bone loss, or body weight in *Sod1*$^{-/-}$ mice (Figure 1C–F).

The XDH-stable-type mutation cannot convert to an XO form, which produces $O_2^{\bullet-}$. We, therefore, expected XDH-stable-type mutations to rescue the aging-like phenotypes via reduction of the $O_2^{\bullet-}$-induced oxidative damage in *Sod1*$^{-/-}$ mice. To further clarify the protective effect of XDH against aging-like pathologies, we also analyzed the tissue changes in *Sod1*$^{-/-}$ XDH-stable-type (C995R) KI double-mutant mice (Figure 2). *Sod1*$^{-/-}$ XDH-stable-type double-mutant mice were born normally without any lethal or apparent growth abnormalities (data not shown). Unexpectedly, XDH-stable type did not improve the hemolytic anemia associated with the splenomegaly induced by SOD1 deficiency (Figure 2A,B). Consistent with the XO-locked type, the XDH-stable type also failed to change the systemic pathologies, including fatty liver, muscle atrophy, bone loss, and low body weight in *Sod1*$^{-/-}$ mice (Figure 2C–F). These results suggest that neither XO nor XDH types of XOR are involved in the various aging-like pathologies induced by SOD1 deficiency.

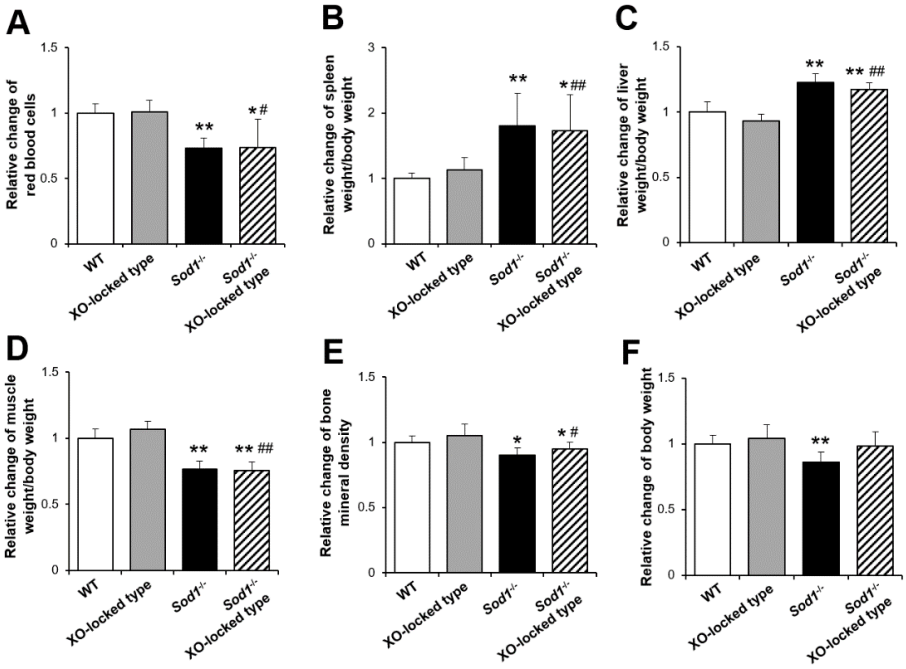

Figure 1. A phenotypical analysis of *Sod1*, xanthine oxidase (XO)-locked-type double-mutant mice. Relative changes in the red blood cell count (**A**), ratio of spleen weight/body weight (**B**), ratio of liver weight/body weight (**C**), ratio of muscle weight/body weight (**D**), bone mineral density (**E**), and body weight (**F**) of wild-type (WT), $Sod1^{-/-}$, XO-locked-type, and $Sod1^{-/-}$ XO-locked-type male and female mice (4–5 months of age, n = 5–6). * $p < 0.05$, ** $p < 0.01$ vs. WT. $^{\#}$ $p < 0.05$, $^{\#\#}$ $p < 0.01$ vs. XO-locked type. Data are shown as the mean ± SD.

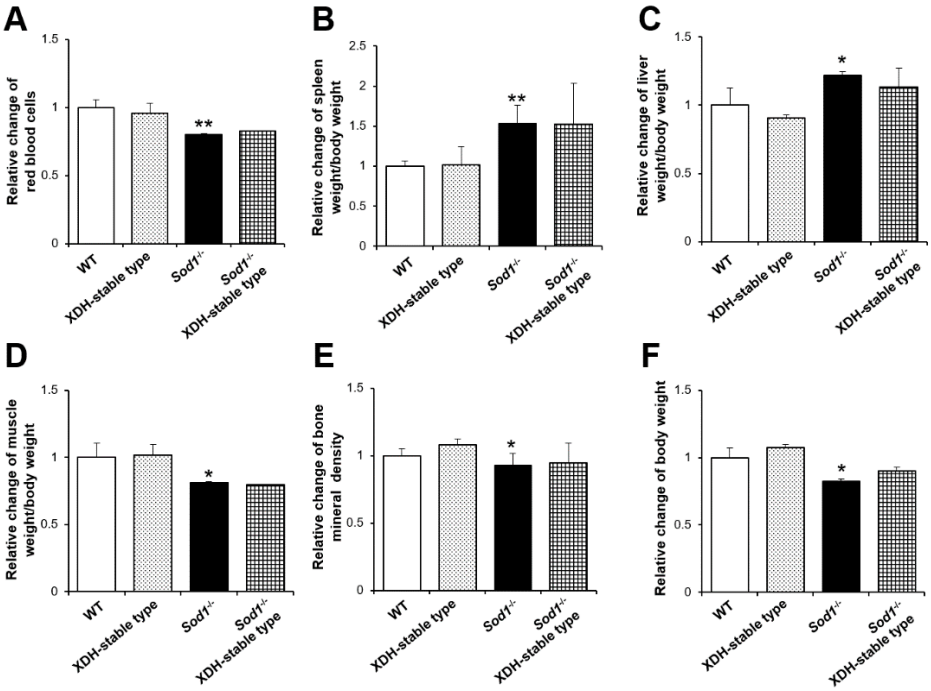

Figure 2. A phenotypical analysis of *Sod1*, XDH-stable-type double-mutant mice. Relative changes in the red blood cell count (**A**), spleen weight (**B**), ratio of spleen weight/body weight (**C**), ratio of muscle weight/body weight (**D**), bone mineral density (**E**), and body weight (**F**) of WT, $Sod1^{-/-}$, XDH-stable, and $Sod1^{-/-}$ XDH-stable male mice (4–5 months of age, n = 3). * $p < 0.05$, ** $p < 0.01$. Data are shown as the mean ± SD.

2.2. XO Inhibitor Fails to Improve the Aging-Like Pathologies in *Sod1*$^{-/-}$ Mice

In vitro studies using rodents have revealed that the administration of allopurinol (30–50 mg/kg/day), an XO inhibitor, via drinking water reduces serum uric acid by 50–90% for 2–14 weeks [28–30]. According to these experimental protocols, we administered allopurinol (30 mg/kg/day) for 8 weeks to determine the improvement effect of XO-derived $O_2^{\bullet-}$ inhibition on tissue degeneration in *Sod1*$^{-/-}$ mice. In wild-type (WT) mice, the administration of allopurinol did not change the body weight, suggesting no noticeable adverse effects (Figure 3A). *Sod1*$^{-/-}$ mice exhibited no significant changes in body weight due to allopurinol administration, and their body weight remained lower than that of WT mice (Figure 3A). Unexpectedly, *Sod1*$^{-/-}$ mice administered allopurinol exhibited significant bone loss, anemia, fatty liver, and muscle and skin atrophy compared with WT mice (Figure 3B–F).

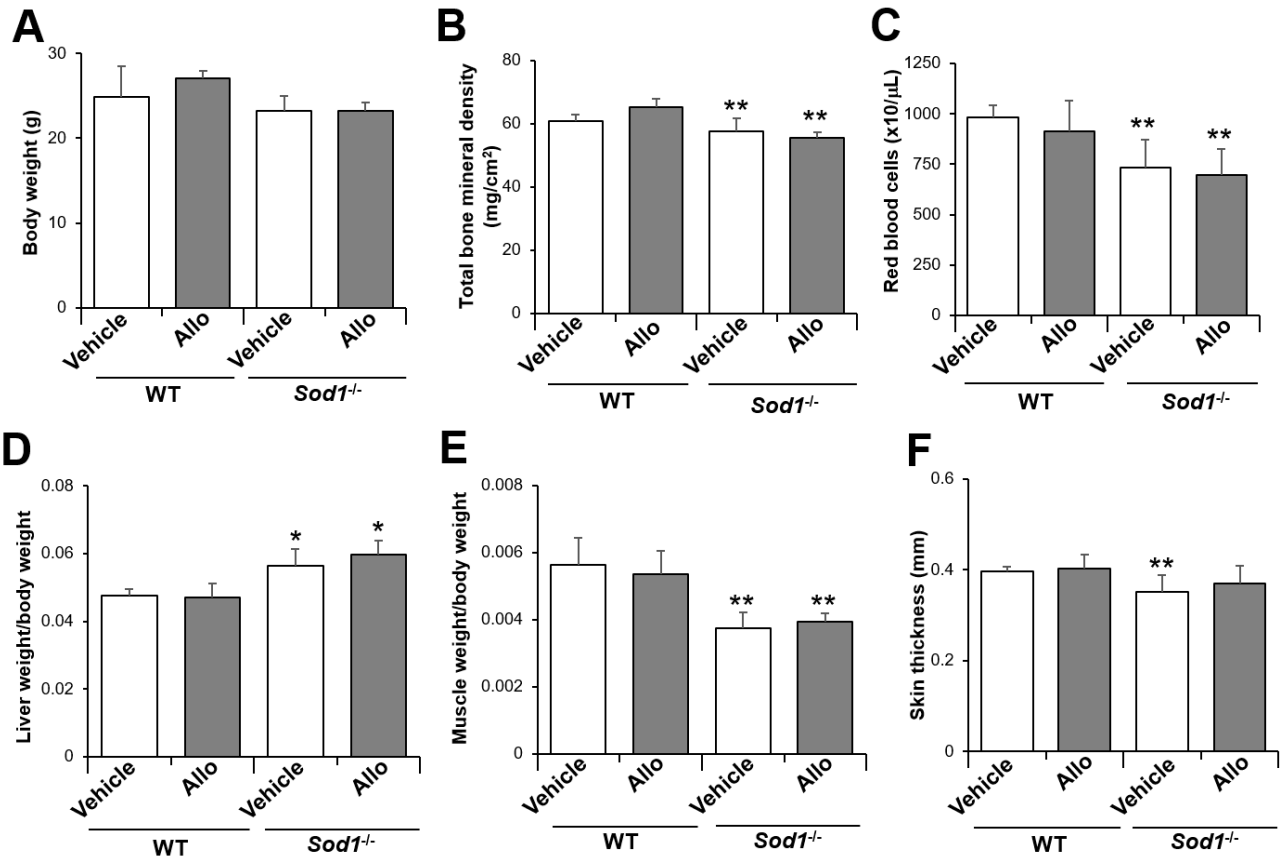

Figure 3. Administration of allopurinol to adult *Sod1*$^{-/-}$ female mice. The body weight (**A**), total bone mineral density (**B**), red blood cell count (**C**), ratio of liver weight/body weight (**D**), ratio of muscle weight/body weight (**E**), and skin thickness (**F**) of WT and *Sod1*$^{-/-}$ female mice (7 months of age, n = 4–5) administered allopurinol for 8 weeks. * $p < 0.05$, ** $p < 0.01$. Data are shown as the mean ± SD.

To investigate the potential effects of sex differences, we also administered allopurinol to *Sod1*$^{-/-}$ male mice. As in female mice, allopurinol did not improve any of these pathologies in *Sod1*$^{-/-}$ male mice (Figure 4). Furthermore, to investigate the contribution of $O_2^{\bullet-}$ derived from other pathways, we also administered apocynin (0.4 g/kg/day), an NOX inhibitor, to *Sod1*$^{-/-}$ mice. Apocynin treatment also failed to improve the systemic aging pathologies in *Sod1*$^{-/-}$ male mice (Figure 4). These results suggest that $O_2^{\bullet-}$ derived from XO and NOX has no association with tissue pathologies in *Sod1*$^{-/-}$ mice.

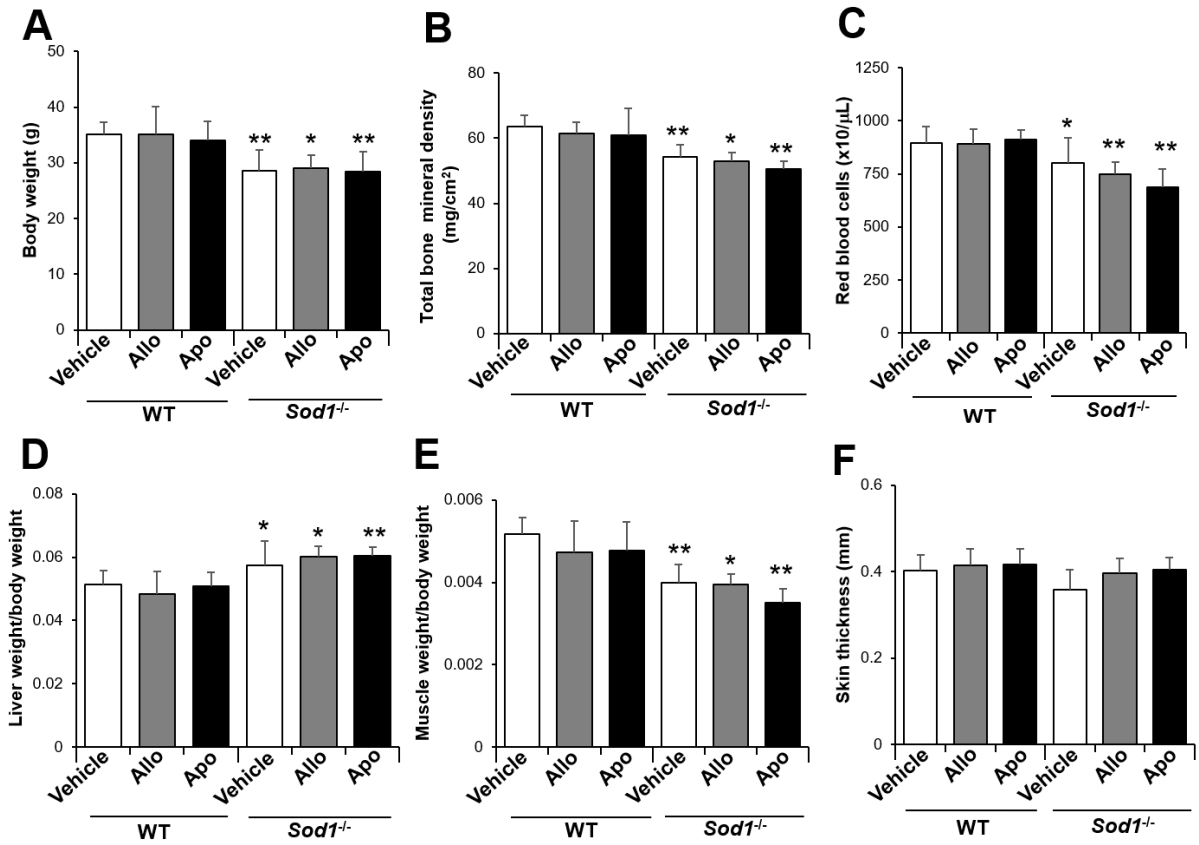

Figure 4. Administration of allopurinol to aged *Sod1*$^{-/-}$ male mice. The body weight (**A**), total bone mineral density (**B**), red blood cell count (**C**), ratio of liver weight/body weight (**D**), ratio of muscle weight/body weight (**E**), and skin thickness (**F**) of WT and *Sod1*$^{-/-}$ male mice (12 months of age, n = 4–5) administered allopurinol or apocynin for 8 weeks. * $p < 0.05$, ** $p < 0.01$. Data are shown as the mean ± SD.

3. Discussion

3.1. Contribution of XO-Derived $O_2^{\bullet-}$ to Tissue Pathology

The two types of KI mice for XO-locked- or XDH-stable TKI mutations are powerful tools for clarifying the pathological effects of XOR in various tissues. In contrast to the therapeutic effects of allopurinol on the tissue pathologies induced by acute injuries [22–25], modulation of XO activity by genetic engineering or pharmacological techniques failed to attenuate aging-associated pathologies induced by *Sod1*$^{-/-}$ mice (Figures 1–4). We also found that apocynin did not alter the tissue pathologies in *Sod1*$^{-/-}$ mice (Figure 4). In an in vitro study, treatment with a mixture of allopurinol, apocynin, and N^{ω}-Nitro-L-arginine methyl ester hydrochloride, an NOS inhibitor, failed to attenuate the ROS accumulation in *Sod1*$^{-/-}$ cells (data not shown). These data strongly suggest that SOD1 does not physiologically catalyze $O_2^{\bullet-}$ derived from XO, NOX, or NOS. Mitochondria produce ROS, including $O_2^{\bullet-}$, through the electron transport chains of complexes I and III and release $O_2^{\bullet-}$ to both sides of the inner mitochondrial membrane [31]. SOD1 is also slightly localized in the intermembrane space of mitochondria in rats and yeast [32–34], suggesting that SOD1 mainly catalyzes $O_2^{\bullet-}$ in the intermembrane space and cytoplasm. In contrast, mitochondrial SOD2 mainly degrades $O_2^{\bullet-}$ in the mitochondrial matrix. Paraquat generates mitochondrial $O_2^{\bullet-}$ via complex I inhibition, resulting in mitochondrial dysfunction [35]. Paraquat treatment actually shortened the life span of *Sod1*$^{-/-}$ mice [36], suggesting that $O_2^{\bullet-}$ derived from mitochondria plays a major role in SOD1-mediated metabolism in cytoplasm. Other mechanisms of ROS production have also been reported, such as via cyclooxygenase, Fenton, and Haber–Weiss reactions mainly generating peroxy and hydroxy radicals [37].

These reactions may contribute slightly but not markedly to SOD1-mediated metabolism in cells.

SOD1 deficiency also increases ROS, proinflammatory cytokines, and lipoperoxides in various organs, including the muscle, skin, liver, and blood [4,15,19,38–41]. The status of redox, inflammation, and lipoperoxides in *Sod1*$^{-/-}$ XOR double-mutant mice should be clarified in future studies. Furthermore, *Sod1*$^{-/-}$ mice exhibited various tissue pathologies, including anemia, fatty liver, muscle atrophy, bone loss, and skin atrophy (Figures 1–4). In contrast, tissue pathologies induced by XO activation occur, especially in the heart, vascular tissue, and nerves [22–25], and do not overlap with affected tissues in *Sod1*$^{-/-}$ mice, suggesting that XO-mediated oxidative damages may show distinct organ selectivity from *Sod1*$^{-/-}$ mice. We recently demonstrated that *Sod1* loss activates the Forkhead box O3–matrix metalloproteinase-2 axis in the skin [42], suggesting that selective signaling pathways are activated by SOD1-catalyzing $O_2^{\bullet -}$ from mitochondria.

In the present study, we were unable to match the age of *Sod1*$^{-/-}$ mice in Figures 1–4. Although we noted no marked difference in the pathological features of *Sod1*$^{-/-}$ mice between 4 and 12 months of age, the results need to be reinvestigated with the same protocols. Since complete SOD1 loss has not been reported in human diseases, the interpretation of our result using knockout mice is limited. A partial inhibition model of SOD1, such as that using an inhibitor, would be valuable for revealing the cross talk between aging-like pathology and $O_2^{\bullet -}$ generation.

3.2. Contribution of XO-Derived O_2^- to Tissue Pathology

XOR catalyzes the reaction steps from hypoxanthine to xanthine and from xanthine to uric acid in the pathway of purine metabolism [20]. Uric acid is also known as the classical radical scavenger, such as singlet oxygen, peroxyl radicals, and hydroxyl radicals [43,44]. Antioxidant activity of uric acid protects the erythrocyte membrane from lipid oxidation [45,46]. Uric acid also improves various pathologies, including sclerosis, Parkinson's disease, acute stroke, ischemia-induced brain injury, allergic encephalomyelitis, doxorubicin-induced cardiotoxicity, and hepatopathy induced by hemorrhagic shock [47–53]. Uric acid itself also generates some radicals and acts as a prooxidant [43]. Uric acid amplified the oxidation of liposomes via peroxynitrite generation [54]. This oxidant–antioxidant paradox of uric acid further complicates our understanding of the contribution of XO to the tissue pathology caused by oxidative stress in *Sod1*$^{-/-}$ mice.

3.3. Pathological Effect of XO on Aging and Tumorigenesis

Aging is also associated with the progressive impairment of homeostasis as a result of chronic redox imbalance and inflammation. XO is upregulated by proinflammatory cytokines, such as tumor necrosis factor-α and interleukin-6 [55]. Indeed, the XO expression and activity have been shown to increase in an age-dependent manner in the liver, kidney, thymus, aorta, and plasma [56–58]. XO-derived $O_2^{\bullet -}$ stimulates activator protein 1 activity via c-jun N-terminal kinase and p38 in vascular smooth muscle [59], suggesting XO as a possible $O_2^{\bullet -}$ donor in inflammation-related pathologies. These reports suggest that $O_2^{\bullet -}$ released from mitochondria causes chronic pathologies, and XO-derived $O_2^{\bullet -}$ induces acute tissue damage.

A high level of ROS leads to the activation of various oncogenic pathways [60]. We previously demonstrated that XO-locked-type KI mice promote tumor growth due to increased ROS production in macrophages [21]. *Sod1*$^{-/-}$ mice also show hepatocarcinogenesis progress associated with the accumulation of oxidative damage in late life stages [3]. To clarify the contribution of SOD1 to tumorigenesis, we generated *Sod1*$^{-/-}$ *p53*$^{-/-}$ double-knockout mice. Compared to *p53*$^{-/-}$ mice, *Sod1*$^{-/-}$ *p53*$^{-/-}$ double-knockout mice showed significantly accelerated tumorigenesis by 4 months of age (Watanabe et al. submitted), suggesting alteration of the tumorigenesis profiles by redox imbalance. Neither *Sod1*$^{-/-}$ XO-locked-type nor *Sod1*$^{-/-}$ XDH-stable-type double-mutant mice exhibited tumor for-

mation in the liver or other tissues at 7–12 months of age (data not shown). At older ages, XO-locked- and XDH-stable-type mutations may alter tumorigenesis in *Sod1*$^{-/-}$ mice. To clarify the contribution of XOR to tumorigenesis in *Sod1*$^{-/-}$ mice, further analyses are needed to characterize the pathogenic macrophages and tumorigenesis in *Sod1*$^{-/-}$ XO-locked-type and *Sod1*$^{-/-}$ XDH-stable-type double-mutant mice.

In conclusion, KI mutations of XOR and inhibitors of XO or NOX did not alter the aging-like pathologies in *Sod1*$^{-/-}$ mice, suggesting that XOR-mediated $O_2^{\bullet-}$ production contributes relatively little to the aging-like pathologies in *Sod1*$^{-/-}$ mice. SOD1 may use $O_2^{\bullet-}$ produced by physiological and biological systems, such as mitochondrial energy production. The production source of $O_2^{\bullet-}$ may affect tissue homeostasis and the optimal therapeutic strategy in ROS-related diseases in humans. Our results provide new insight into the pathophysiological role of $O_2^{\bullet-}$ in oxygen metabolism by SOD and XOR.

4. Materials and Methods

4.1. Animals and Genotyping

Sod1$^{-/-}$ mice were purchased from the Jackson Laboratory (Bar Harbor, ME, USA). Genotyping of the *Sod1*$^{-/-}$ allele was performed via genomic polymerase chain reaction using genomic DNA isolated from the tail tip, as reported previously [14]. Two Xdh gene-modified mice, the XO-locked (W338A/F339L mutant) and the XDH-stable (C995R mutant) types [21], were kindly provided by Drs. Teruo Kusano, Takeshi Nishino (Nippon Medical School, Bunkyo-ku, Japan), and Ken Okamoto (The University of Tokyo, Bunkyo-ku, Japan). These animals were housed under a 12 h/12 h light/dark cycle and fed ad libitum. In addition, they were maintained and studied according to the protocols approved by the animal care committee of Chiba University and the National Center for Geriatrics and Gerontology.

4.2. Administration of Allopurinol and Apocynin

The WT and *Sod1*$^{-/-}$ mice were given 1 mM allopurinol (30 mg/kg/day, 09-12502; FUJIFILM Wako Pure Chemical Corporation, Osaka, Japan) and 2 mg/mL of apocynin (0.4 g/ kg/day, 6002; EXTRASYNTHASE, Metropole de Lyon, France) in drinking water daily for 8 weeks from 7 weeks of age (female) and 12 weeks of age (male).

4.3. Analysis of Aging-Like Pathologies

Red blood cells were measured using Celltac a (MEK-6358; NIHON KODEN, Shinjuku-ku, Japan). Bone mineral density of the whole body was measured using a PIXImus instrument (Lunar Corp., Madison, WI, USA). The thickness of the isolated back skin was measured using a PEACOCK dial thickness gauge (OZAKI MFG. CO., LTD., Itabashi-ku, Japan).

4.4. Statistical Analyses

Statistical analyses were performed using one-way analysis of variance/Tukey's test for comparisons of three or more groups. Differences between data were considered significant when p-values were less than 0.05. All data are expressed as the mean ± standard deviation (SD).

Author Contributions: S.S. and T.S. designed the study. S.S. and T.S. wrote the manuscript. S.S., K.W., and Y.O. performed the research. S.S. and K.W. analyzed the data. S.S., K.W., and T.S. discussed the hypothesis and interpreted the data. S.S. and T.S. edited the article. T.S. coordinated and directed the project. All authors have read and agreed to the published version of the manuscript.

Funding: This research was supported by a fund from the Gout and Uric Acid Foundation of Japan and the National Center for Geriatrics and Gerontology.

Institutional Review Board Statement: All experiments involving animals were performed according to protocols approved by the animal care committee of Chiba University (G26-26 and A28-258) and the National Center for Geriatrics and Gerontology (G2-28 and A3-10).

Informed Consent Statement: Not applicable.

Acknowledgments: We thank Teruo Kusano, Takeshi Nishino (Nippon Medical School), and Ken Okamoto (The University of Tokyo) for supplying the XO-locked- and XDH-stable-type KI mice. We also thank Daichi Morikawa and Toshihiko Toda (Chiba University) for their valuable technical assistance.

Conflicts of Interest: The authors declare no conflict of interest in association with the present study.

Abbreviations

ROS	Reactive oxygen species
$O_2^{\bullet -}$	Superoxide
XOR	Xanthine oxidoreductase
NADPH	Nicotinamide adenine dinucleotide phosphate
NOX	NADPH oxidase
NO	Nitric oxide
SOD	Superoxide dismutase
Sod1$^{-/-}$	*Sod1*-deficient
XO	Xanthin oxidase
XDH	Xanthin dehydrogenase
KI	Knock-in
WT	Wild type

References

1. Finkel, T.; Holbrook, N.J. Oxidants, oxidative stress and the biology of ageing. *Nature* **2000**, *408*, 239–247. [CrossRef] [PubMed]
2. Li, J.M.; Shah, A.M. Endothelial cell superoxide generation: Regulation and relevance for cardiovascular pathophysiology. *Am. J. Physiol. Regul. Integr. Comp. Physiol.* **2004**, *287*, 1014–1030. [CrossRef] [PubMed]
3. Elchuri, S.; Oberley, T.D.; Qi, W.; Eisenstein, R.S.; Jackson Roberts, L.; Van Remmen, H.; Epstein, C.J.; Huang, T.T. CuZnSOD deficiency leads to persistent and widespread oxidative damage and hepatocarcinogenesis later in life. *Oncogene* **2005**, *24*, 367–380. [CrossRef]
4. Uchiyama, S.; Shimizu, T.; Shirasawa, T. CuZn-SOD deficiency causes ApoB degradation and induces hepatic lipid accumulation by impaired lipoprotein secretion in mice. *J. Biol. Chem.* **2006**, *281*, 31713–31719. [CrossRef]
5. Murakami, K.; Murata, N.; Noda, Y.; Tahara, S.; Kaneko, T.; Kinoshita, N.; Hatsuta, H.; Murayama, S.; Barnham, K.J.; Irie, K.; et al. SOD1 (copper/zinc superoxide dismutase) deficiency drives amyloid beta protein oligomerization and memory loss in mouse model of Alzheimer disease. *J. Biol. Chem.* **2011**, *286*, 44557–44568. [CrossRef]
6. Murakami, K.; Murata, N.; Noda, Y.; Irie, K.; Shirasawa, T.; Shimizu, T. Stimulation of the amyloidogenic pathway by cytoplasmic superoxide radicals in an Alzheimer's disease mouse model. *Biosci. Biotechnol. Biochem.* **2012**, *76*, 1098–1103. [CrossRef]
7. Imamura, Y.; Noda, S.; Hashizume, K.; Shinoda, K.; Yamaguchi, M.; Uchiyama, S.; Shimizu, T.; Mizushima, Y.; Shirasawa, T.; Tsubota, K. Drusen, choroidal neovascularization, and retinal pigment epithelium dysfunction in SOD1-deficient mice: A model of age-related macular degeneration. *Proc. Natl. Acad. Sci. USA* **2006**, *103*, 11282–11287. [CrossRef]
8. Hashizume, K.; Hirasawa, M.; Imamura, Y.; Noda, S.; Shimizu, T.; Shinoda, K.; Kurihara, T.; Noda, K.; Ozawa, Y.; Ishida, S.; et al. Retinal dysfunction and progressive retinal cell death in SOD1-deficient mice. *Am. J. Pathol.* **2008**, *172*, 1325–1331. [CrossRef]
9. Kojima, T.; Wakamatsu, T.H.; Dogru, M.; Ogawa, Y.; Igarashi, A.; Ibrahim, O.M.; Inaba, T.; Shimizu, T.; Noda, S.; Obata, H.; et al. Age-related dysfunction of the lacrimal gland and oxidative stress: Evidence from the Cu,Zn-superoxide dismutase-1 (Sod1) knockout mice. *Am. J. Pathol.* **2012**, *180*, 1879–1896. [CrossRef]
10. Ibrahim, O.M.; Dogru, M.; Matsumoto, Y.; Igarashi, A.; Kojima, T.; Wakamatsu, T.H.; Inaba, T.; Shimizu, T.; Shimazaki, J.; Tsubota, K. Oxidative stress induced age dependent meibomian gland dysfunction in cu, zn-superoxide dismutase-1 (sod1) knockout mice. *PLoS ONE* **2014**, *9*, e99328. [CrossRef]
11. Iuchi, Y.; Okada, F.; Onuma, K.; Onoda, T.; Asao, H.; Kobayashi, M.; Fujii, J. Elevated oxidative stress in erythrocytes due to a SOD1 deficiency causes anaemia and triggers autoantibody production. *Biochem. J.* **2007**, *402*, 219–227. [CrossRef]
12. Nojiri, H.; Saita, Y.; Morikawa, D.; Kobayashi, K.; Tsuda, C.; Miyazaki, T.; Saito, M.; Marumo, K.; Yonezawa, I.; Kaneko, K.; et al. Cytoplasmic superoxide causes bone fragility owing to low-turnover osteoporosis and impaired collagen cross-linking. *J. Bone Miner. Res.* **2011**, *26*, 2682–2694. [CrossRef] [PubMed]
13. Morikawa, D.; Nojiri, H.; Saita, Y.; Kobayashi, K.; Watanabe, K.; Ozawa, Y.; Koike, M.; Asou, Y.; Takaku, T.; Kaneko, K.; et al. Cytoplasmic reactive oxygen species and SOD1 regulate bone mass during mechanical unloading. *J. Bone Miner. Res.* **2013**, *28*, 2368–2380. [CrossRef] [PubMed]
14. Murakami, K.; Inagaki, J.; Saito, M.; Ikeda, Y.; Tsuda, C.; Noda, Y.; Kawakami, S.; Shirasawa, T.; Shimizu, T. Skin atrophy in cytoplasmic SOD-deficient mice and its complete recovery using a vitamin C derivative. *Biochem. Biophys. Res. Commun.* **2009**, *382*, 457–461. [CrossRef] [PubMed]

15. Shibuya, S.; Ozawa, Y.; Toda, T.; Watanabe, K.; Tometsuka, C.; Ogura, T.; Koyama, Y.; Shimizu, T. Collagen peptide and vitamin C additively attenuate age-related skin atrophy in Sod1-deficient mice. *Biosci. Biotechnol. Biochem.* **2014**, *78*, 1212–1220. [CrossRef]
16. Muller, F.L.; Song, W.; Liu, Y.; Chaudhuri, A.; Pieke-Dahl, S.; Strong, R.; Huang, T.T.; Epstein, C.J.; Roberts, L.J., 2nd; Csete, M.; et al. Absence of CuZn superoxide dismutase leads to elevated oxidative stress and acceleration of age-dependent skeletal muscle atrophy. *Free Radic. Biol. Med.* **2006**, *40*, 1993–2004. [CrossRef]
17. Noda, Y.; Ota, K.; Shirasawa, T.; Shimizu, T. Copper/zinc superoxide dismutase insufficiency impairs progesterone secretion and fertility in female mice. *Biol. Reprod.* **2012**, *86*, 1–8. [CrossRef]
18. Sagi, H.; Shibuya, S.; Kato, T.; Nakanishi, Y.; Tsuboi, A.; Moriya, S.; Ohno, H.; Miyamoto, H.; Kodama, H.; Shimizu, T. SOD1 deficiency alters gastrointestinal microbiota and metabolites in mice. *Exp. Gerontol.* **2020**, *130*, 110795. [CrossRef] [PubMed]
19. Watanabe, K.; Shibuya, S.; Ozawa, Y.; Nojiri, H.; Izuo, N.; Yokote, K.; Shimizu, T. Superoxide dismutase 1 loss disturbs intracellular redox signaling, resulting in global age-related pathological changes. *BioMed Res. Int.* **2014**, *2014*, 140165. [CrossRef] [PubMed]
20. Okamoto, K.; Kusano, T.; Nishino, T. Chemical nature and reaction mechanisms of the molybdenum cofactor of xanthine oxidoreductase. *Curr. Pharm. Des.* **2013**, *19*, 2606–2614. [CrossRef]
21. Kusano, T.; Ehirchiou, D.; Matsumura, T.; Chobaz, V.; Nasi, S.; Castelblanco, M.; So, A.; Lavanchy, C.; Acha-Orbea, H.; Nishino, T.; et al. Targeted knock-in mice expressing the oxidase-fixed form of xanthine oxidoreductase favor tumor growth. *Nat. Commun.* **2019**, *10*, 4904. [CrossRef]
22. Brown, J.M.; Terada, L.S.; Grosso, M.A.; Whitmann, G.J.; Velasco, S.E.; Patt, A.; Harken, A.H.; Repine, J.E. Xanthine oxidase produces hydrogen peroxide which contributes to reperfusion injury of ischemic, isolated, perfused rat hearts. *J. Clin. Investig.* **1988**, *81*, 1297–1301. [CrossRef] [PubMed]
23. Terada, L.S.; Rubinstein, J.D.; Lesnefsky, E.J.; Horwitz, L.D.; Leff, J.A.; Repine, J.E. Existence and participation of xanthine oxidase in reperfusion injury of ischemic rabbit myocardium. *Am. J. Physiol.* **1991**, *260*, 805–810. [CrossRef] [PubMed]
24. Luo, J.; Yan, D.; Li, S.; Liu, S.; Zeng, F.; Cheung, C.W.; Liu, H.; Irwin, M.G.; Huang, H.; Xia, Z. Allopurinol reduces oxidative stress and activates Nrf2/p62 to attenuate diabetic cardiomyopathy in rats. *J. Cell. Mol. Med.* **2020**, *24*, 1760–1773. [CrossRef]
25. Baloglu, M.; Gokalp Ozkorkmaz, E. Neuroprotective effects of allopurinol on spinal cord injury in rats: A biochemical and immunohistochemical study. *Folia Morphol.* **2019**, *78*, 676–683. [CrossRef] [PubMed]
26. Vorbach, C.; Scriven, A.; Capecchi, M.R. The housekeeping gene xanthine oxidoreductase is necessary for milk fat droplet enveloping and secretion: Gene sharing in the lactating mammary gland. *Genes Dev.* **2002**, *16*, 3223–3235. [CrossRef]
27. Nasi, S.; Castelblanco, M.; Chobaz, V.; Ehirchios, D.; So, A.; Bernabei, I.; Kusano, T.; Nishino, T.; Okamoto, K.; Busso, N. Xanthine oxidoreductase Is involved in chondrocyte mineralization and expressed in osteoarthritic damaged cartilage. *Front. Cell. Dev. Biol.* **2021**, *9*, 612440. [CrossRef] [PubMed]
28. Kosugi, T.; Nakayama, T.; Heinig, M.; Zhang, L.; Yuzawa, Y.; Sanchez-Lozada, L.G.; Roncal, C.; Johnson, R.J.; Nakagawa, T. Effect of lowering uric acid on renal disease in the type 2 diabetic db/db mice. *Am. J. Physiol. Renal. Physiol.* **2009**, *297*, 481–488. [CrossRef]
29. Derbre, F.; Ferrando, B.; Gomez-Cabrera, M.C.; Sanchis-Gomar, F.; Martinez-Bello, V.E.; Olaso-Gonzalez, G.; Diaz, A.; Gratas-Delamarche, A.; Cerda, M.; Vina, J. Inhibition of xanthine oxidase by allopurinol prevents skeletal muscle atrophy: Role of p38 MAPKinase and E3 ubiquitin ligases. *PLoS ONE* **2012**, *7*, e46668. [CrossRef]
30. Kato, S.; Shirakami, Y.; Yamaguchi, K.; Mizutani, T.; Ideta, T.; Nakamura, H.; Ninomiya, S.; Kubota, M.; Sakai, H.; Ibuka, T.; et al. Allopurinol suppresses azoxymethane-induced colorectal tumorigenesis in C57BL/KsJ-db/db mice. *Gastrointest. Disord.* **2020**, *2*, 35. [CrossRef]
31. Muller, F.L.; Liu, Y.; Van Remmen, H. Complex III releases superoxide to both sides of the inner mitochondrial membrane. *J. Biol. Chem.* **2004**, *279*, 49064–49073. [CrossRef]
32. Okado-Matsumoto, A.; Fridovich, I. Subcellular distribution of superoxide dismutases (SOD) in rat liver: Cu,Zn-SOD in mitochondria. *J. Biol. Chem.* **2001**, *276*, 38388–38393. [CrossRef] [PubMed]
33. Sturtz, L.A.; Diekert, K.; Jensen, L.T.; Lill, R.; Culotta, V.C. A fraction of yeast Cu,Zn-superoxide dismutase and its metallochaperone, CCS, localize to the intermembrane space of mitochondria. A physiological role for SOD1 in guarding against mitochondrial oxidative damage. *J. Biol. Chem.* **2001**, *276*, 38084–38089. [CrossRef]
34. Tsang, C.K.; Liu, Y.; Thomas, J.; Zhang, Y.; Zheng, X.F. Superoxide dismutase 1 acts as a nuclear transcription factor to regulate oxidative stress resistance. *Nat. Commun.* **2014**, *5*, 3446. [CrossRef] [PubMed]
35. Cocheme, H.M.; Murphy, M.P. Complex I is the major site of mitochondrial superoxide production by paraquat. *J. Biol. Chem.* **2008**, *283*, 1786–1798. [CrossRef] [PubMed]
36. Ho, Y.S.; Gargano, M.; Cao, J.; Bronson, R.T.; Heimler, I.; Hutz, R.J. Reduced fertility in female mice lacking copper-zinc superoxide dismutase. *J. Biol. Chem.* **1998**, *273*, 7765–7769. [CrossRef]
37. Snezhkina, A.V.; Kudryavtseva, A.V.; Kardymon, O.L.; Savvateeva, M.V.; Melnikova, N.V.; Krasnov, G.S.; Dmitriev, A.A. ROS generation and antioxidant defense systems in normal and malignant cells. *Oxid. Med. Cell. Longev.* **2019**, *2019*, 6175804. [CrossRef]
38. Shibuya, S.; Ozawa, Y.; Watanabe, K.; Izuo, N.; Toda, T.; Yokote, K.; Shimizu, T. Palladium and platinum nanoparticles attenuate aging-like skin atrophy via antioxidant activity in mice. *PLoS ONE* **2014**, *9*, e109288. [CrossRef] [PubMed]
39. Qaisar, R.; Bhaskaran, S.; Ranjit, R.; Sataranatarajan, K.; Premkumar, P.; Huseman, K.; Van Remmen, H. Restoration of SERCA ATPase prevents oxidative stress-related muscle atrophy and weakness. *Redox Biol.* **2019**, *20*, 68–74. [CrossRef]

40. Jang, Y.C.; Rodriguez, K.; Lustgarten, M.S.; Muller, F.L.; Bhattacharya, A.; Pierce, A.; Choi, J.J.; Lee, N.H.; Chaudhuri, A.; Richardson, A.G.; et al. Superoxide-mediated oxidative stress accelerates skeletal muscle atrophy by synchronous activation of proteolytic systems. *Geroscience* **2020**, *42*, 1579–1591. [CrossRef]
41. Bhaskaran, S.; Pollock, N.; Macpherson, P.C.; Ahn, B.; Piekarz, K.M.; Staunton, C.A.; Brown, J.L.; Qaisar, R.; Vasilaki, A.; Richardson, A.; et al. Neuron-specific deletion of CuZnSOD leads to an advanced sarcopenic phenotype in older mice. *Aging Cell.* **2020**, *19*, e13225. [CrossRef]
42. Kim, J.; Toda, T.; Watanabe, K.; Shibuya, S.; Ozawa, Y.; Izuo, N.; Cho, S.; Seo, D.B.; Yokote, K.; Shimizu, T. Syringaresinol Reverses Age-Related Skin Atrophy by Suppressing FoxO3a-Mediated Matrix Metalloproteinase-2 Activation in Copper/Zinc Superoxide Dismutase-Deficient Mice. *J. Investig. Dermatol.* **2019**, *139*, 648–655. [CrossRef]
43. Sautin, Y.Y.; Johnson, R.J. Uric acid: The oxidant-antioxidant paradox. *Nucleosides Nucleotides Nucleic Acids* **2008**, *27*, 608–619. [CrossRef] [PubMed]
44. El Ridi, R.; Tallima, H. Physiological functions and pathogenic potential of uric acid: A review. *J. Adv. Res.* **2017**, *8*, 487–493. [CrossRef]
45. Ames, B.N.; Cathcart, R.; Schwiers, E.; Hochstein, P. Uric acid provides an antioxidant defense in humans against oxidant- and radical-caused aging and cancer: A hypothesis. *Proc. Natl. Acad. Sci. USA* **1981**, *78*, 6858–6862. [CrossRef] [PubMed]
46. Zavaroni, I.; Mazza, S.; Fantuzzi, M.; Dall'Aglio, E.; Bonora, E.; Delsignore, R.; Passeri, M.; Reaven, G.M. Changes in insulin and lipid metabolism in males with asymptomatic hyperuricaemia. *J. Intern. Med.* **1993**, *234*, 25–30. [CrossRef]
47. Amaro, S.; Soy, D.; Obach, V.; Cervera, A.; Planas, A.M.; Chamorro, A. A pilot study of dual treatment with recombinant tissue plasminogen activator and uric acid in acute ischemic stroke. *Stroke* **2007**, *38*, 2173–2175. [CrossRef]
48. Duan, W.; Ladenheim, B.; Cutler, R.G.; Kruman, I.I.; Cadet, J.L.; Mattson, M.P. Dietary folate deficiency and elevated homocysteine levels endanger dopaminergic neurons in models of Parkinson's disease. *J. Neurochem.* **2002**, *80*, 101–110. [CrossRef] [PubMed]
49. Hooper, D.C.; Spitsin, S.; Kean, R.B.; Champion, J.M.; Dickson, G.M.; Chaudhry, I.; Koprowski, H. Uric acid, a natural scavenger of peroxynitrite, in experimental allergic encephalomyelitis and multiple sclerosis. *Proc. Natl. Acad. Sci. USA* **1998**, *95*, 675–680. [CrossRef]
50. Spitsin, S.V.; Scott, G.S.; Mikheeva, T.; Zborek, A.; Kean, R.B.; Brimer, C.M.; Koprowski, H.; Hooper, D.C. Comparison of uric acid and ascorbic acid in protection against EAE. *Free Radic. Biol. Med.* **2002**, *33*, 1363–1371. [CrossRef]
51. Yu, Z.F.; Bruce-Keller, A.J.; Goodman, Y.; Mattson, M.P. Uric acid protects neurons against excitotoxic and metabolic insults in cell culture, and against focal ischemic brain injury in vivo. *J. Neurosci. Res.* **1998**, *53*, 613–625. [CrossRef]
52. Tsukada, K.; Hasegawa, T.; Tsutsumi, S.; Katoh, H.; Kuwano, H.; Miyazaki, T.; Yamamoto, Y. Effect of uric acid on liver injury during hemorrhagic shock. *Surgery* **2000**, *127*, 439–446. [CrossRef]
53. Wang, J.; Fan, Y.; Cai, X.; Gao, Z.; Yu, Z.; Wei, B.; Tang, Y.; Hu, L.; Liu, W.T.; Gu, Y. Uric acid preconditioning alleviated doxorubicin induced JNK activation and Cx43 phosphorylation associated cardiotoxicity via activation of AMPK-SHP2 signaling pathway. *Ann. Transl. Med.* **2020**, *8*, 1570. [CrossRef]
54. Santos, C.X.; Anjos, E.I.; Augusto, O. Uric acid oxidation by peroxynitrite: Multiple reactions, free radical formation, and amplification of lipid oxidation. *Arch. Biochem. Biophys.* **1999**, *372*, 285–294. [CrossRef] [PubMed]
55. Komaki, Y.; Sugiura, H.; Koarai, A.; Tomaki, M.; Ogawa, H.; Akita, T.; Hattori, T.; Ichinose, M. Cytokine-mediated xanthine oxidase upregulation in chronic obstructive pulmonary disease's airways. *Pulm. Pharmacol. Ther.* **2005**, *18*, 297–302. [CrossRef] [PubMed]
56. Chung, H.Y.; Song, S.H.; Kim, H.J.; Ikeno, Y.; Yu, B.P. Modulation of renal xanthine oxidoreductase in aging: Gene expression and reactive oxygen species generation. *J. Nutr. Health Aging* **1999**, *3*, 19–23. [PubMed]
57. Newaz, M.A.; Yousefipour, Z.; Oyekan, A. Oxidative stress-associated vascular aging is xanthine oxidase-dependent but not NAD(P)H oxidase-dependent. *J. Cardiovasc. Pharmacol.* **2006**, *48*, 88–94. [CrossRef] [PubMed]
58. Vida, C.; Rodriguez-Teres, S.; Heras, V.; Corpas, I.; De la Fuente, M.; Gonzalez, E. The aged-related increase in xanthine oxidase expression and activity in several tissues from mice is not shown in long-lived animals. *Biogerontology* **2011**, *12*, 551–564. [CrossRef] [PubMed]
59. Matesanz, N.; Lafuente, N.; Azcutia, V.; Martin, D.; Cuadrado, A.; Nevado, J.; Rodriguez-Manas, L.; Sanchez-Ferrer, C.F.; Peiro, C. Xanthine oxidase-derived extracellular superoxide anions stimulate activator protein 1 activity and hypertrophy in human vascular smooth muscle via c-Jun N-terminal kinase and p38 mitogen-activated protein kinases. *J. Hypertens.* **2007**, *25*, 609–618. [CrossRef] [PubMed]
60. Schieber, M.; Chandel, N.S. ROS function in redox signaling and oxidative stress. *Curr. Biol.* **2014**, *24*, 453–462. [CrossRef]